

Electronic Supplementary Information

NIR laser scanning microscopy for photophysical characterization of upconversion nanoparticles and nanohybrids

Juan Ferrera-González,^{*a} Laura Francés-Soriano,^{a,b} Nestor Estébanez,^a Enrique Navarro-Raga,^c María González-Béjar^{*a} and Julia Pérez-Prieto^{*1}

^a Instituto de Ciencia Molecular (ICMol), Departamento de Química Orgánica, University of Valencia, C/ Catedrático José Beltrán, 2, Paterna, Valencia 46980, Spain

^b nanoFRET.com, Laboratoire COBRA (Chimie Organique, Bioorganique, Réactivité et Analyse), Université de Rouen Normandie, CNRS, INSA, 76821 Mont-Saint-Aignan Cedex, France

^c Servicio Central de Soporte a la Investigación Experimental (SCSIE). University of Valencia, Burjassot, Valencia 46100, Spain

CONTENT

Instruments and methods.....	2
Experimental.....	2
Estimation of lifetime window.....	3
Estimation of excitation energy.....	3
Figure S1. EDX spectra from UC _{Er,2} , UC _{Er,20} , UC _{Tm} and UC _{Ho}	4
Table S1. Composition of UC _{Er,2} , UC _{Er,20} , UC _{Tm} and UC _{Ho} from EDX.....	4
Figure S2. TEM images of UC _{Er,2} , UC _{Er,20} , UC _{Tm} and UC _{Ho}	5
Figure S3. XRD diffractogram UC _{Er,2} , UC _{Er,20} , UC _{Tm} and UC _{Ho}	5
Figure S4. Absorption spectra of UC _{Tm} @Rh101 and UC _{Tm} @Rh110.....	6
Figure S5. SEM images of the UC _{Er,2}	6
Figure S6. NIR-LSM image of UC _{Er,20} in channel 2.....	7
Figure S7. Fitted kinetic of UC _{Tm} @Rh110 agglomerate.....	7
Table S2. Decay lifetimes of UC _{Er,2} , UC _{Er,20} , UC _{Tm} and UC _{Ho}	7
Figure S8. NIR-LSM image of C1 and C2 of UC _{Tm} @Rh110 exciting at 975 nm	8
Table S3. Decay lifetimes obtained for bare-UC _{Tm} and UC _{Tm} @Rh110.....	8
Figure S9. NIR-LSM images exciting at 975 nm and at 1030 nm UC _{Tm} @Rh101 sample.....	8
Figure S10. Colocalization analysis of UC _{Tm} @Rh101.....	9
Figure S11. Colocalization analysis of UC _{Tm} @Rh110.....	9
Figure S12. NIR-LSM Intensity profile of Tm emission vs. dye emission of UC _{Tm} @Rh110.....	10
Estimation of spatial resolution.....	10
Figure S13. Visualization of pixel, laser spot, nanoparticles and aggregates sizes.....	10
References.....	10

Instruments and methods

UV-vis spectroscopy

The UV-visible-NIR spectra of the colloidal UCNHs were recorded in a UV/Vis/NIR spectrophotometer Lambda 1050 Perkin Elmer.

TEM images

TEM images were obtained using a Jeol 1010 microscope operating at 100 kV equipped with an AMT RX80 (8 Mpx) charge-coupled device (CCD) camera. For the preparation of the UCNP samples, 10 μL of a 0.5 $\text{mg}\cdot\text{mL}^{-1}$ solution of the UCNP was left to dry under vacuum at room temperature on a formvar/carbon film supported on a 300-mesh copper grid. High-resolution transmission electron microscopy (HRTEM) images were recorded using a TECNAI G2 F20 microscope operating at 200 kV (point resolution of 0.24 nm) and equipped with a Gatan Multiscan 794 (1 Mpx) CCD camera.

SEM images

Scanning electron microscopy (SEM) images were obtained using Field emission microscope HITACHI S-4800, working at 20 kV. The UCNP samples were deposited in a glass slide by spin coating as explained above.

EDX analysis

The energy dispersive X-ray spectroscopy (EDX) analysis was acquired using a scanning electron microscope HITACHI S-4800 equipped with XFlash 5030 Bruker detector and acquisition software QUANTAX 400. The UCNP samples were deposited on adhesive carbon tape.

XRD

XRD diffractograms were registered on a Bruker D8 Advance A25 diffractometer using $\text{CuK}\alpha$ ($\lambda = 1.54060 \text{ \AA}$) radiation at a voltage of 40 kV and 30 mA, and a LynxEye detector. The powder diffraction pattern was scanned over the angular range of 2-80° (2 θ) with a step size of 0.020°, at room temperature.

Image processing and statistical analysis in colocalization

Image processing was performed with the open source software ImageJ/FIJI.¹ Background levels were equilibrated in the whole image by subtracting a median filtered image.² Colocalization coefficients and significance tests were calculated by the ImageJ GDSC Plugin which performs the Confined Displacement Algorithm (CDA).³ The ROI of each image was obtained by applying the Otsu threshold and the confined compartment is the entire image (Figs. S10 and S11). Clipping signal (saturated) was discarded for the analysis. For visualization purposes the brightness of the images showed in the main subscript has been magnified.

Experimental

Materials

Chemicals: The chemicals used for the synthesis of the nanoparticles were: lanthanide chlorides ($\text{YCl}_3\cdot 6\text{H}_2\text{O}$, $\text{YbCl}_3\cdot 6\text{H}_2\text{O}$, $\text{ErCl}_3\cdot 6\text{H}_2\text{O}$, $\text{TmCl}_3\cdot 6\text{H}_2\text{O}$ and $\text{HoCl}_3\cdot 6\text{H}_2\text{O}$ (>99.9%, all of them)), 1-octadecene (95%), oleic acid (70%), NaOH and NH_4F (99.99%). All these chemicals were purchased from Sigma-Aldrich used as received without previous purification.

Synthesis

Synthesis of oleate-capped $\text{NaYF}_4\text{:Yb}^{3+}$ (15%), Er^{3+} (2%) and $\text{NaYF}_4\text{:Yb}^{3+}$ (16%), Er^{3+} (18%) nanoparticles ($\text{UC}_{\text{Er},2}$, $\text{UC}_{\text{Er},20}$).

$\text{NaYF}_4\text{:Yb,Er}$ nanoparticles were synthesized by following a previously reported protocol with some modifications.⁴ In a 50 mL round-bottom flask, oleic acid (8 mL) and octadecene (15 mL) were added. Then, a solution containing $\text{YCl}_3\cdot 6\text{H}_2\text{O}$ (0.78 mmol or 0.60 mmol), $\text{YbCl}_3\cdot 6\text{H}_2\text{O}$ (0.20 mmol for the two syntheses) and $\text{ErCl}_3\cdot 6\text{H}_2\text{O}$ (0.02 mmol or 0.20 mmol) dissolved in methanol (2 mL) was added to the flask and the mixture was stirred at 160 °C under N_2 until everything was dissolved. Next, the solution was cooled to 100 °C and 10 mL of a methanol solution containing NaOH (2.5 mmol) and NH_4F (4.0 mmol) were slowly added into the flask during 5 min. Then the solution was heated until 125 °C under N_2 flow and continuous stirring to remove completely methanol and water traces. Finally, the reaction was heated at 305 °C under N_2 flux for one hour. After that, the solution was cooled to room temperature and the nanoparticles were precipitated by centrifugation (9000 rpm, 15 min, 25 °C). Later on, the oleate-capped UCNP were washed three times with (43.5:40.5:16 v/v) hexane/acetone/methanol solution and once with ethanol. As usual, the Y:Yb:Er ratio used in the preparation (78, 20, 2 and 60, 20, 20 % respectively) is slightly different than the proportion obtained in EDS analyses of the final UC_{Er} (83, 15, 2 and 66, 16, 18 %).

Synthesis of oleate-capped $\text{NaYF}_4\text{:Yb}^{3+}$ (17%), Tm^{3+} (0.2%) nanoparticles (UC_{Tm}).

$\text{NaYF}_4\text{:Yb,Tm}$ nanoparticles were synthesized by following a previously reported protocol with some modifications.⁴ In a 50 mL round-bottom flask, oleic acid (8 mL) and octadecene (15 mL) were added. Then, a solution containing $\text{YCl}_3\cdot 6\text{H}_2\text{O}$ (0.80 mmol),

YbCl₃·6H₂O (0.20 mmol), TmCl₃·6H₂O (0.002 mmol) dissolved in methanol (2 mL) was added to the flask and the mixture was stirred at 160 °C under N₂ until everything was dissolved. Next, the solution was cooled to 100 °C and 10 mL of a methanol solution containing NaOH (2.5 mmol) and NH₄F (4.0 mmol) were slowly added into the flask during 5 min. Then the solution was heated until 125 °C under N₂ flow and continuous stirring to remove completely methanol and water traces. Finally, the reaction was heated at 305 °C under N₂ flux for one hour. After that, the solution was cooled to room temperature and the nanoparticles were precipitated by centrifugation (9000 rpm, 15 min, 25 °C). Later on, the oleate-capped UCNPs were washed three times with (43.5:40.5:16 v/v) hexane/acetone/methanol solution and once with ethanol. As usual, the Y: Yb:Tm ratio used in the preparation (80, 20 and 0.2 % respectively) is slightly different than the proportion obtained in EDS analyses of the final UC_{Tm} (83, 17 and <1).

Synthesis of oleate-capped NaYF₄:Yb³⁺ (19%), Ho³⁺ (1.0%) nanoparticles (UC_{Ho}).

NaYF₄:Yb, Ho nanoparticles were synthesized by following the same protocol used in the synthesis of the UCNPs doped with erbium and thulium described above.⁴ In a 50 mL round-bottom-flask, oleic acid (8 mL) and octadecene (15 mL) were added. Then, a solution containing YCl₃·6H₂O (0.79 mmol), YbCl₃·6H₂O (0.20 mmol), HoCl₃·6H₂O (0.10 mmol) dissolved in methanol (2 mL) was added to the flask and the mixture was stirred at 160 °C under N₂ until everything was dissolved. Next, the solution was cooled to 100 °C and 10 mL of a methanol solution containing NaOH (2.5 mmol) and NH₄F (4.0 mmol) were slowly added into the flask during 5 min. Then the solution was heated until 125 °C under N₂ flow and continuous stirring to remove completely methanol and water traces. Finally, the reaction was heated at 305 °C under N₂ flux for one hour. After that, the solution was cooled to room temperature and the nanoparticles were precipitated by centrifugation (9000 rpm, 15 min, 25 °C). Later on, the oleate-capped UCNPs were washed three times with (43.5:40.5:16 v/v) hexane/acetone/methanol solution and once with ethanol.

Estimation of lifetime window

The minimum and maximum lifetime (τ) than can be estimated with NIR-LSM have been calculated assuming a monoexponential decay by the following equations:

$$\tau_{min} (\mu s) = \frac{d_{min} \cdot Px}{t_w}$$

$$\tau_{max} (\mu s) = \frac{d_{max} \cdot Px_{max}}{t_w}$$

Where d_{min} and d_{max} are minimum and maximum dwell times, Px is the minimum number of points (pixels) needed to describe an exponential decay (we assumed 10), Px_{max} is the maximum number of pixels per line (4096) and t_w is the optimum temporal window (10); i.e. temporal window should not be shorter than 10 times the lifetime of the emitter.

Estimation of excitation energy

The excitation energy is expressed as the total energy density (fluence) delivered during the dwell time (F_d). It depends on the laser average output power, the excitation wavelength (which defines the diffraction limited laser spot), the laser transmissivity of the acousto-optic modulator, the objective transmission, the objective numerical aperture, the particle size (only if bigger than the pixel size) and the dwell time.

F_d is estimated by measuring the laser power average in the objective port (without the objective) with a thermal sensor (3A-PF-12 Ophir; we measured 220.6 and 482.5 mW at 975 and 800 nm, respectively) and considering the objective transmittance ($\approx 80\%$ at 975 nm), laser transmittance and dwell time. The laser transmittance is changed by a software-controlled (FV10-ASW) acousto-optic modulator which allows for 0.1 – 100% laser transmissivity, 0.1% increments.

The laser spot area (S) is obtained assuming a Gaussian profile, which is perfectly collimated and focused on a spot limited by diffraction and that the objective lenses are free of aberrations. In this way, we can approximate the size of the spot to the Airy disk corrected by an M^2 factor of 1.1.

Finally, the energy density ($J \cdot cm^{-2}$) was calculated by dividing E (J) by S (cm^2):

$$F_d = \frac{E}{S} = \frac{P \cdot \frac{LT}{100} \cdot \frac{OT}{100} \cdot d}{\pi \cdot \left(\frac{0.61 \cdot \lambda_{exc} \cdot 1.1}{NA} \right)^2}$$

P: Laser average power at a certain excitation wavelength (W)

LT: Laser transmission, software controlled (%)

OT: Objective transmission, from specifications (%)

d: dwell time (s/pixel)

λ_{exc} : excitation wavelength (cm)

NA: objective numerical aperture

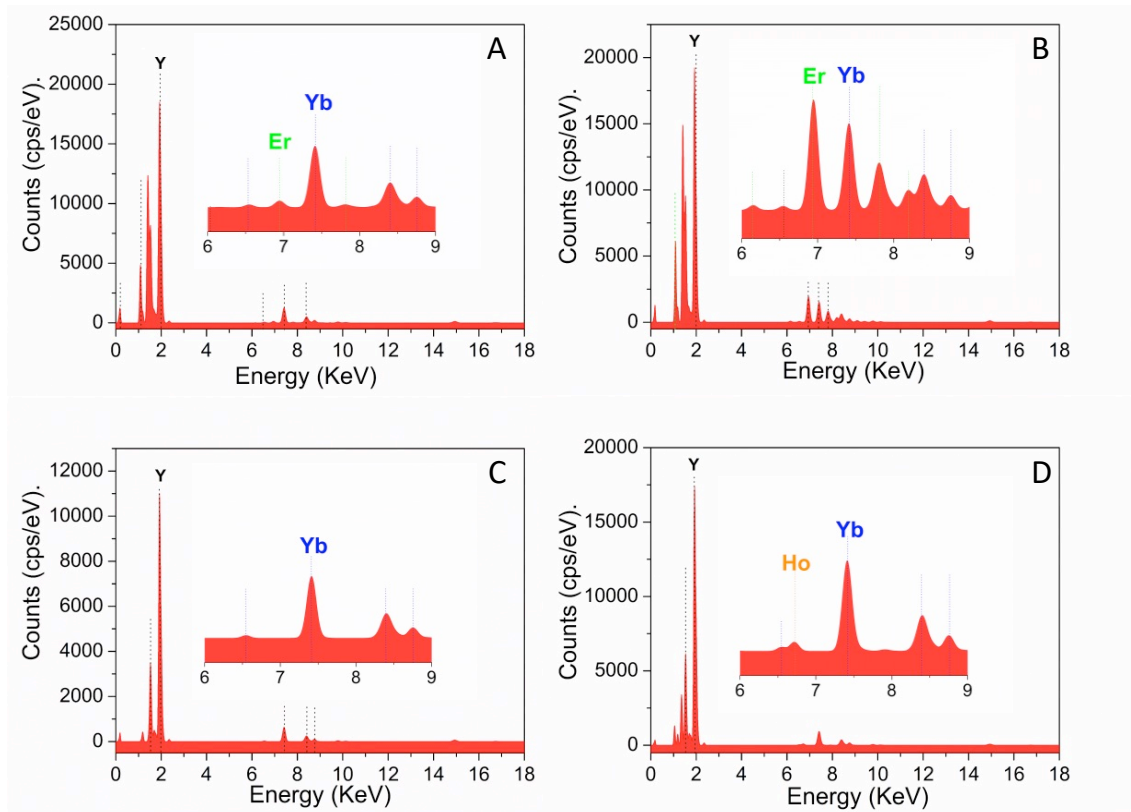


Figure S1. EDX spectra of (A) $UC_{Er,2}: NaYF_4:Yb (20\%), Er(2\%)$; (B) $UC_{Er,20}: NaYF_4:Yb (20\%), Er(20\%)$; (C) $UC_{Tm}: NaYF_4:Yb (20\%), Tm(0.1\%)$ and (D) $UC_{Ho}: NaYF_4:Yb (20\%), Ho(1\%)$.

Table S1. Composition of the samples from EDX (20 Kv)

Sample	Atom. C[at%]				
	Yttrium	Ytterbium	Erbium	Thulium	Holmium
NaYF₄:Yb (20%),Er (2%)	83.3 ± 1.1	15.2 ± 0.2	1.5 ± 0.1	-	-
NaYF₄:Yb(20%),Er(20%)	66.6 ± 2.3	15.7 ± 1.2	17.7 ± 1.3	-	-
NaYF₄:Yb(20%),Tm(0.1%)	82.7 ± 0.9	17.0 ± 0.6	-	<LOD(<1)	-
NaYF₄:Yb(20%),Ho(1%)	79.8 ± 2.1	19.1 ± 0.5	-	-	1.1 ± 0.2

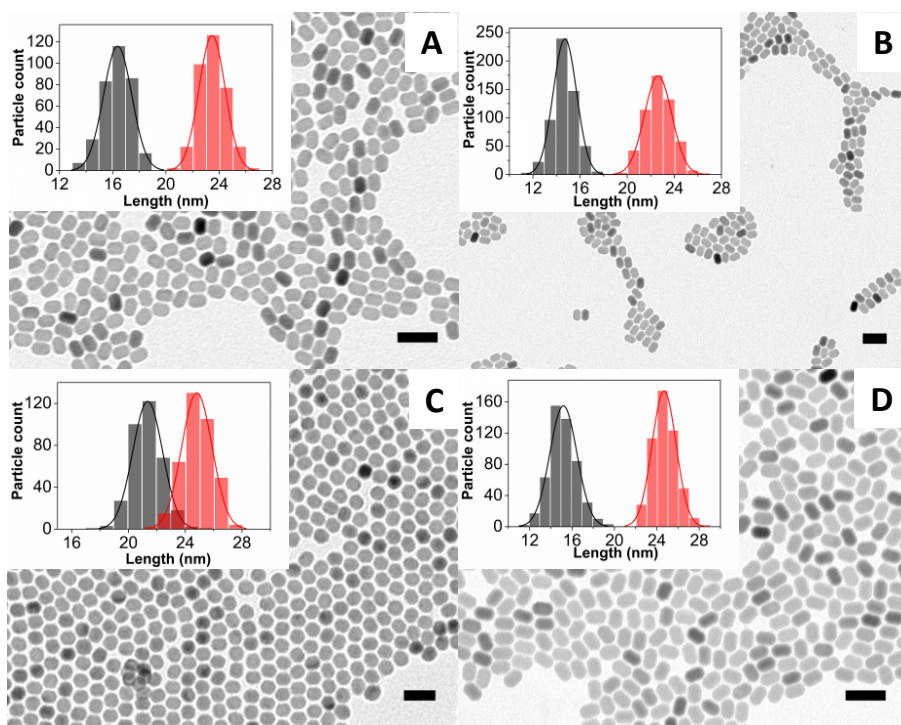


Figure S2. TEM images of (A) UC_{Er,2}, (B) UC_{Er,20}, (C) UC_{Ho} and (D) UC_{Tm}. Scale bar: 50 nm.

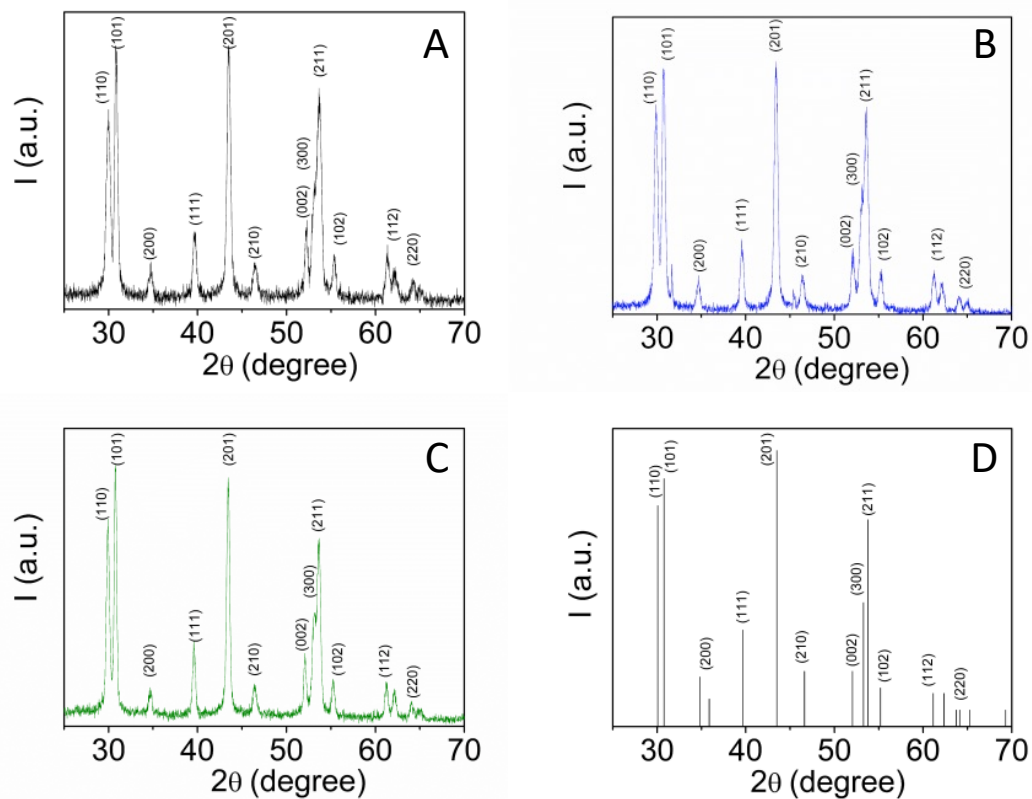


Figure S3. X-ray diffraction (XRD) diffractogram of (A) UC_{Er,2}, (B) UC_{Ho}, (C) UC_{Tm} and (D) hexagonal NaYF₄ standard (JCPDS PDF number 16-0334).

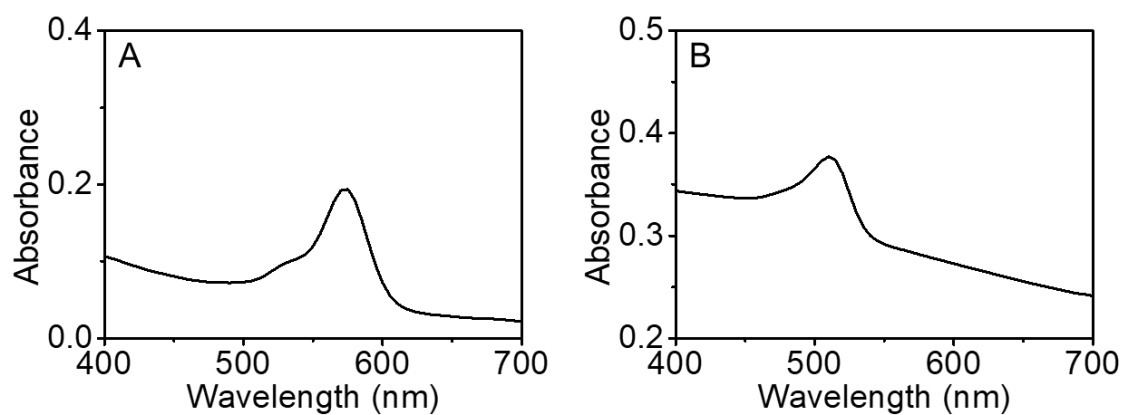


Figure S4. Absorption spectra of the UCNH in DMF (1 mg/mL): (A) UC_{Tm}@Rh101 and (B) UC_{Tm}@Rh110.

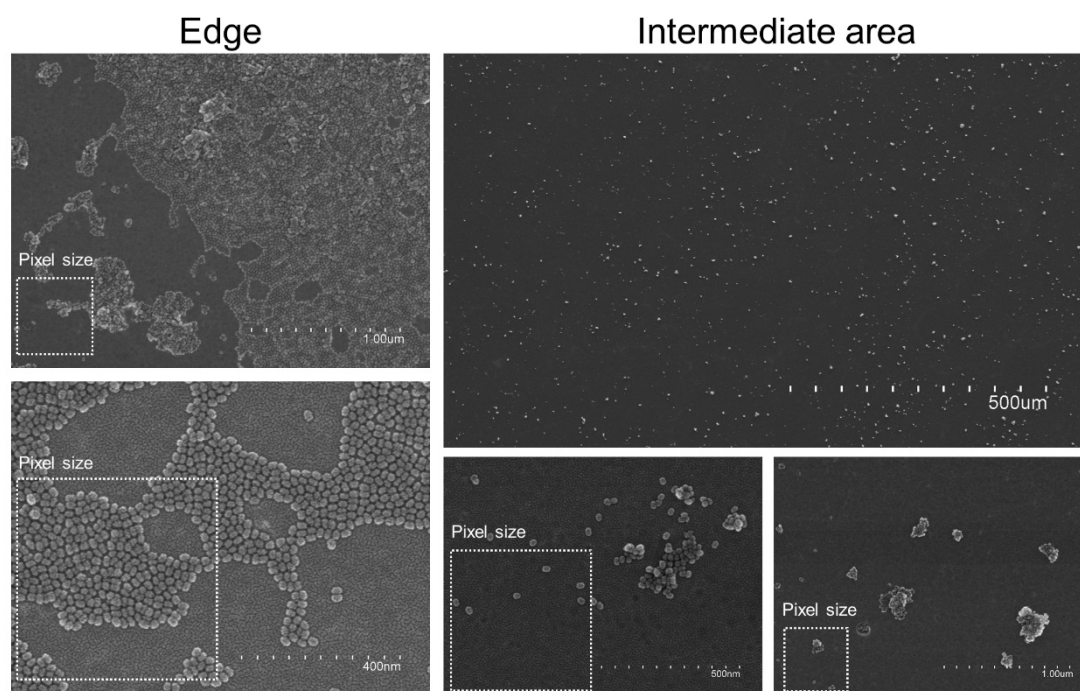


Figure S5. SEM images of the UC_{Er,2} sample displaying different agglomerates and individual UC_{Er,2} on the glass surface. The microscope slide edges showed a higher concentration of UCNPs while intermediate areas were optimal to focus on the NIR-LSM. For comparative purposes, the pixel size (0.5 x 0.5 µm²) is included in each of the NIR-LSM images.

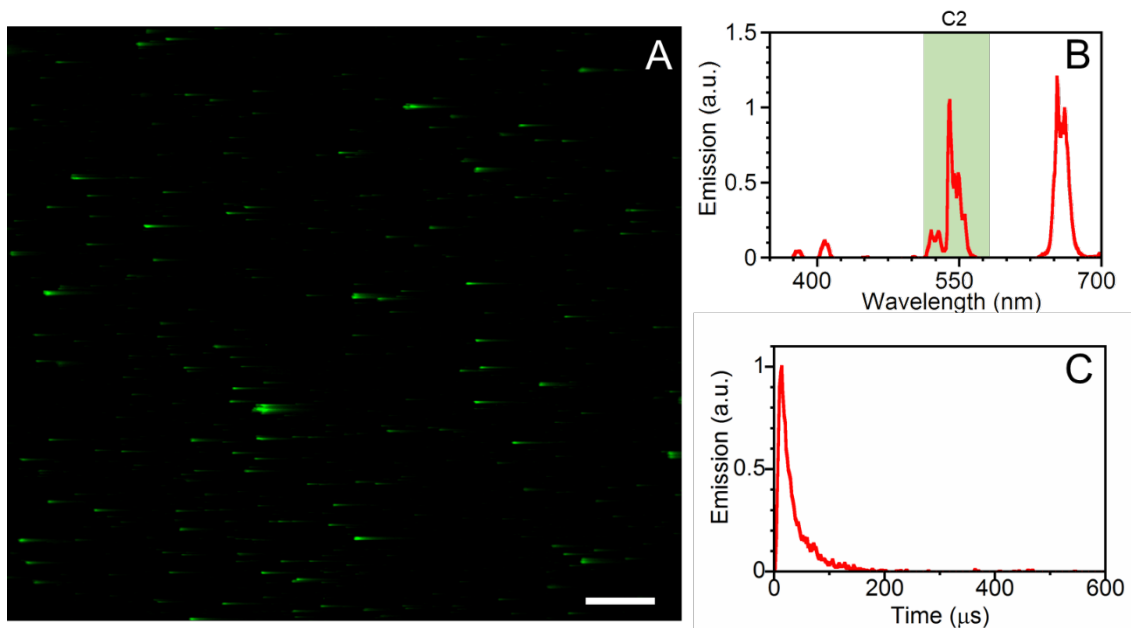
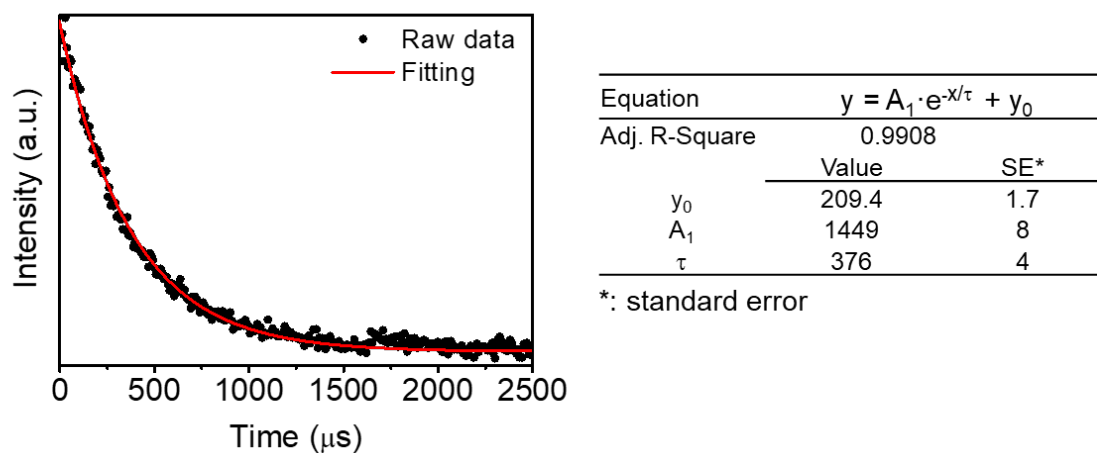


Figure S6. (A) NIR-LSM image of UC_{Er,20} in channel 2 (C2: 515-580 nm; 2 μs·pixel⁻¹; λ_{exc}= 975 nm; F_d= 0.2 J·cm⁻²). Scale bar: 50 μm. (B) Emission spectrum of UC_{Er,20} (λ_{exc}= 975 nm; I= 93 W·cm⁻²). (C) Kinetic profile obtained of a tail in figure A.



5Figure S7. Fitted kinetic of UC_{Tm}@Rh110 (C1: 420-500 nm, λ_{exc}= 975 nm, F_d= 18.4 J·cm⁻²).

Table S2. Comparison of the acquisition conditions and decay lifetime values obtained from the different UCNPs at λ_{exc}= 975 nm (F_d= 0.2 J·cm⁻²).

Sample	Emission (nm)	Dwell time (μs·px ⁻¹)	Decay lifetime (μs)
UC _{Er,2}	515-580	2	68.5 ± 1.1
UC _{Er,20}	515-580	2	22.5 ± 1.5
UC _{Ho}	515-580	2	220.2 ± 2.5
UC _{Tm}	420-500	4	549.4 ± 26.8

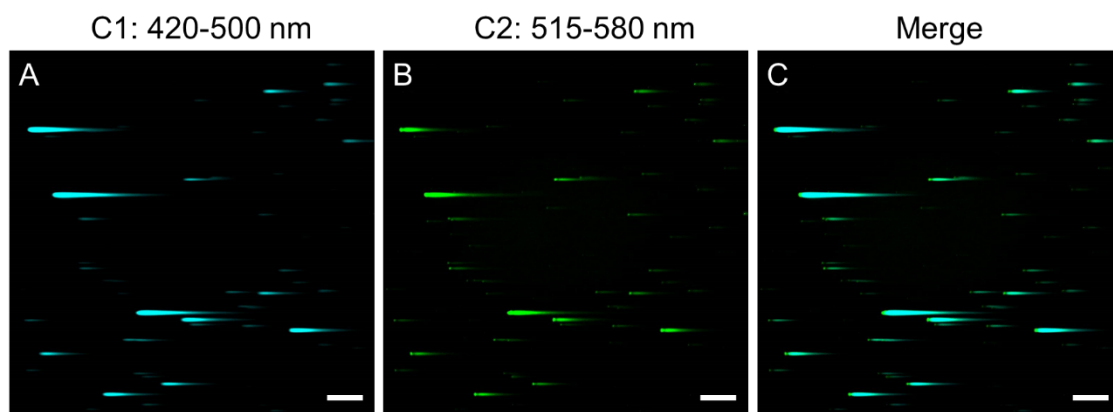


Figure S8. Images of the UCNH UC_{Tm}@Rh110 excited at 975 nm at 8 μs/pixel dwell time in (A) C1, (B) C2 and (C) the composite of both images ($F_d=20.8 \text{ J}\cdot\text{cm}^{-2}$).

Table S3. Decay lifetimes obtained for bare-UC_{Tm} and UC_{Tm}@Rh110 ($\lambda_{\text{exc}}=975 \text{ nm}$; $F_d=18.4 \text{ J}\cdot\text{cm}^{-2}$).

Detection Channel	bare-UC _{Tm}	UC _{Tm} @Rh110
	Decay (SD)	Decay (SD)
C1	403.1 (12.4)	379.9 (15.9)
C2		213.7 (10.0)

SD: standard deviation.

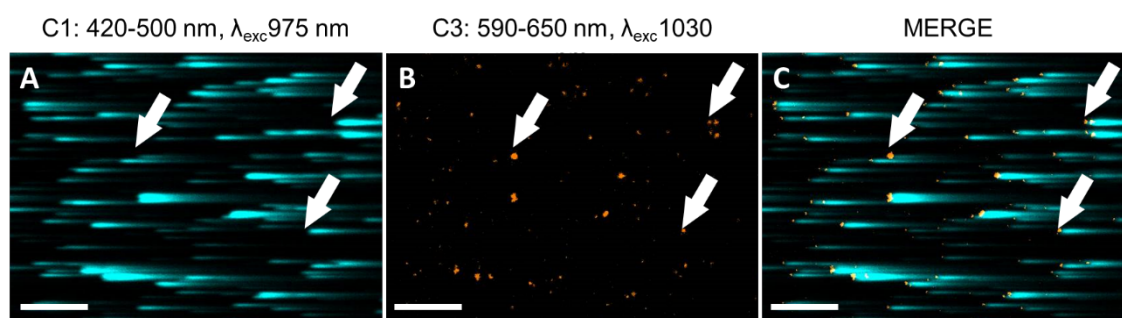


Figure S9. Brightness magnified images of the same region of UC_{Tm}@Rh101 obtained under (A) 975 nm excitation and 10 μs/pixel dwell time ($F_d=21.7 \text{ J}\cdot\text{cm}^{-2}$), and (B) 1030 nm excitation and 10 μs/pixel dwell time ($F_d=22 \text{ J}\cdot\text{cm}^{-2}$). (C) shows both images merged; scale bar 50 μm.

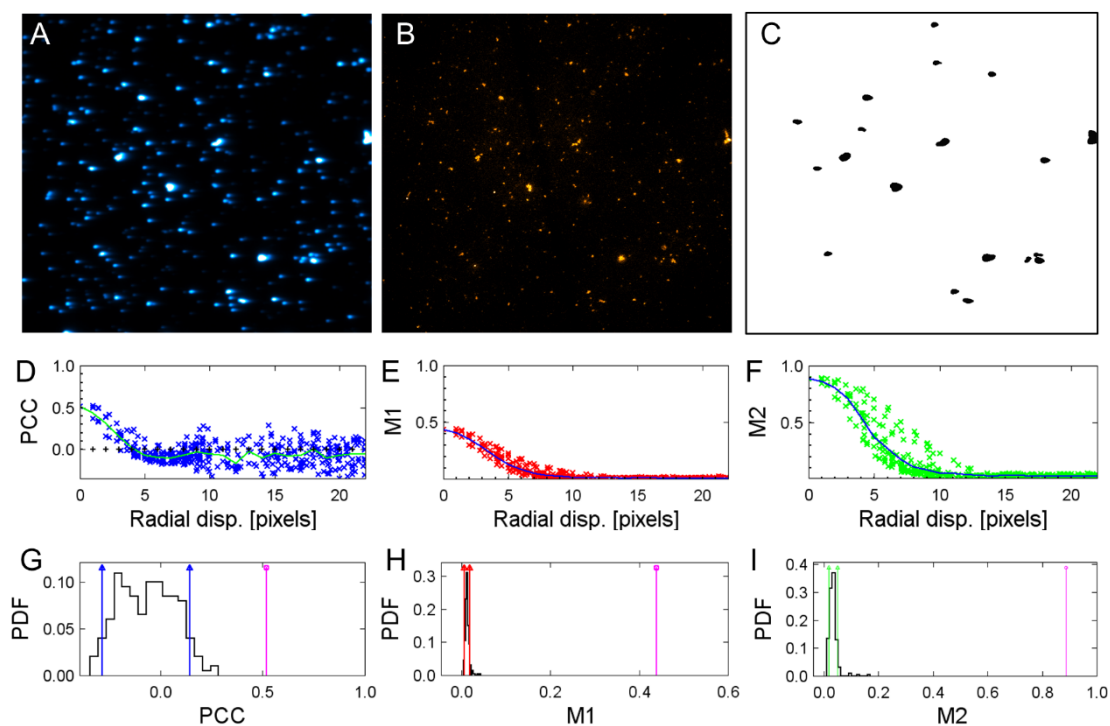


Figure S10. Colocalization analysis of $UC_{Tm}@Rh101$. (A) Raw image obtained in the C1 while exciting at 975 nm and 100 $\mu\text{s}/\text{pixel}$ dwell time ($F_d=218.5 \text{ J}\cdot\text{cm}^{-2}$). (B) Raw image obtained in the C3 while exciting at 1030 nm and 12.5 $\mu\text{s}/\text{pixel}$ dwell time ($F_d=27.5 \text{ J}\cdot\text{cm}^{-2}$). (C) Region of confined compartment (white) used for significance testing. Saturated agglomerates were discarded (black areas). Behavior of individual coefficients PCC (D), M1 (E) and M2 (F2) versus the radial displacement (translations) performed by the CDA algorithm. The probability density function of the coefficients PCC (G), M1 (H) and M2 (I) between 10 to 22 radial displacement. The 95% of confidence interval is shown between colored arrows (blue, red and green for PCC, M1 and M2, respectively) while the original value appears as a pink line. Values obtained were significant.

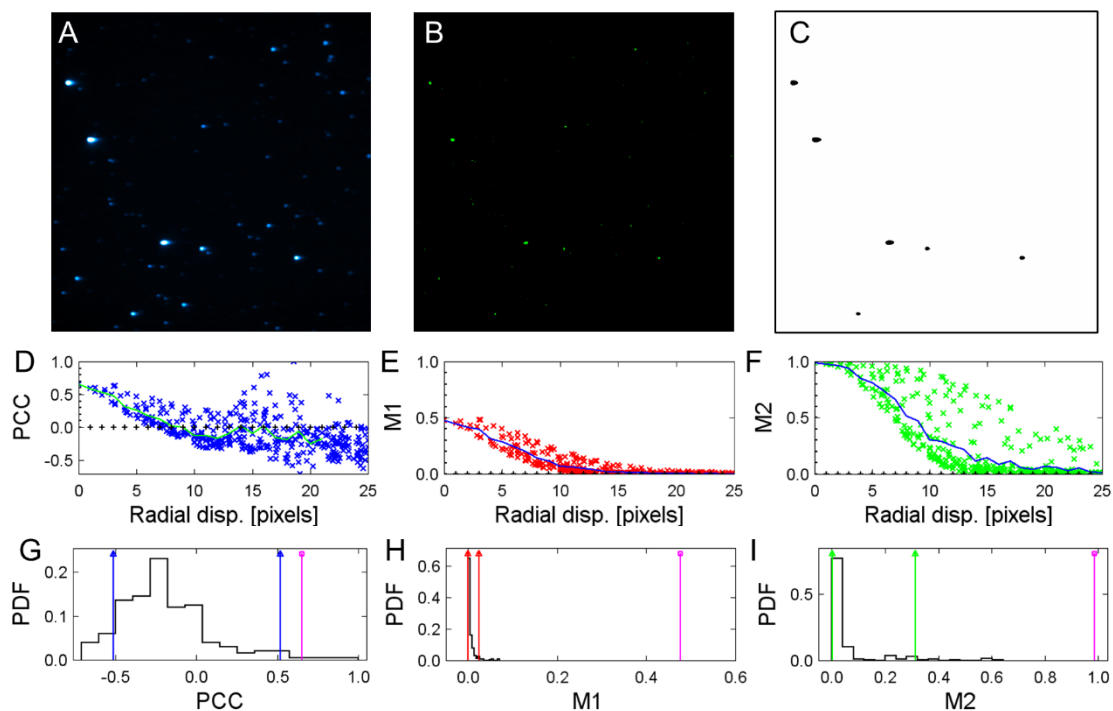


Figure S11. Colocalization analysis of $UC_{Tm}@Rh110$. (A) Raw image obtained in the C1 while exciting at 975 nm and 100 $\mu\text{s}/\text{pixel}$ dwell time ($F_d=260.5 \text{ J}\cdot\text{cm}^{-2}$). (B) Raw image obtained in the C2 while exciting at 1020 nm and 2 $\mu\text{s}/\text{pixel}$ dwell time ($F_d=4.4 \text{ J}\cdot\text{cm}^{-2}$). (C) Region of confined compartment (white) used for significance testing. Saturated agglomerates were discarded (black areas). Behavior of individual coefficients PCC (D), M1 (E) and M2 (F2) versus the radial displacement (translations) performed by the CDA algorithm. The probability density function of the coefficients PCC (G), M1 (H) and M2 (I) between 15 to 25 radial displacement. The 95% of confidence interval is shown between colored arrows (blue, red and green for PCC, M1 and M2, respectively) while the original value appears as pink line. Values obtained were significant.

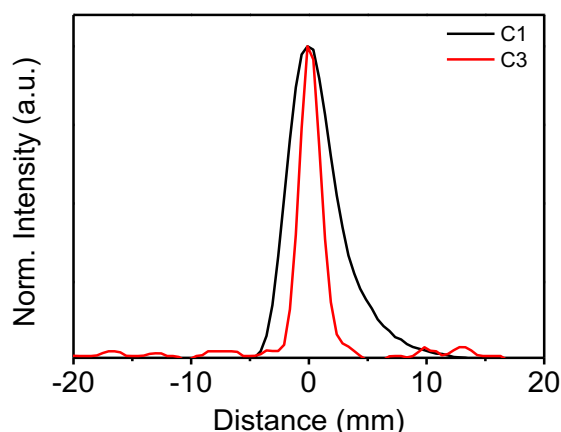


Figure S12. Intensity profile of a random agglomerate of UC_{7m}@Rh101 in the scan direction which causes an underestimation of M1. Black profile was obtained in the detection channel 1 (C1: 420-500 nm) by exciting at 975 nm at 100 $\mu\text{s}/\text{pixel}$ and red profile was obtained in the detection channel 3 (C3: 590-650 nm) by exciting at 1030 nm at 12.5 $\mu\text{s}/\text{pixel}$.

Estimation of spatial resolution

The spatial resolution has been determined according to the Rayleigh criterion of confocal microscopes and afforded a lateral resolution of 473.6 nm.

We are exciting with a spot which covers 2 pixels in the x-axis (1 pixel and two half pixels, Fig. S13), therefore this will be the maximum lateral resolution. In fact, as shown in Figure S12, we would have two different resolutions in a sample: the resolution of the multiphoton excitation of the dye and the resolution of the UCNPs emission.

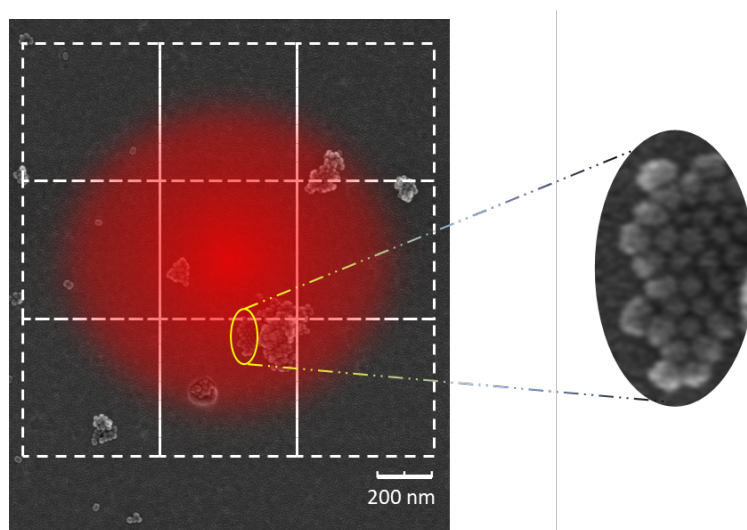


Figure S13. Schematic representation to scale of pixel size (white dashed squares, $0.5 \times 0.5 \mu\text{m}^2$) and diffraction-limited 975 nm laser spot (red circle, $\phi = 1.13 \mu\text{m}$) over a SEM image of the nanoparticles sample. Yellow ellipse has been zoomed in to show a set of close-lying UCNPs.

References:

- 1 J. Schindelin, I. Arganda-Carreras, E. Frise, V. Kaynig, M. Longair, T. Pietzsch, S. Preibisch, C. Rueden, S. Saalfeld, B. Schmid, J.-Y. Tinevez, D. J. White, V. Hartenstein, K. Eliceiri, P. Tomancak and A. Cardona, *Nat. Methods*, 2012, **9**, 676–682.
- 2 K. W. Dunn, M. M. Kamocka and J. H. McDonald, *Am. J. Physiol. - Cell Physiol.*, 2011, **300**, 723–742.
- 3 O. Ramírez, A. García, R. Rojas, A. Couve and S. Härtel, *J. Microsc.*, 2010, **239**, 173–183.
- 4 Z. Li and Y. Zhang, *Nanotechnology*, 2008, **19**, 16–21.
- 5 V. Muhr, C. Würth, M. Kraft, M. Buchner, A. J. Baeumner, U. Resch-Genger and T. Hirsch, *Anal. Chem.*, 2017, **89**, 4868–4874.